이학석사 학위논문

사이아나이드 이온 검출을 위한 수용성 케모센서 개발

Water-soluble Chemosensors for the Colorimetric Detection of Cyanide Ions

울산대학교 대학원

화 학 과

고 영 승

Water-soluble Chemosensors for the Colorimetric Detection of Cyanide Ions

지도교수 이 형 일

이 논문을 이학석사학위 논문으로 제출함

2021년 02월

울 산 대 학 교 대 학 원

화 학 과

고 영 승

고영승의 석사학위 논문을 인준함

심사위원 이형일 인

심사위원 우상국 인

심사위원 이승구 인

울 산 대 학 교 대 학 원

2021년 02월

Abstract

Molecular probes based on hemicyanine group containing electron-donating or electron-withdrawing functional groups (-OCH_3, -H, 3-vinyl, -CH_3, -NO_2, and -CF_3) were synthesized. The probes could detect CN^- ions with high selectivity and sensitivity by changing the color to colorless or turbidimetric response in water. The color change to colorless was clearly observed, indicating that intramolecular charge transfer (ICT) was prevented due to nucleophilic addition of CN^- to the indolium group of probe. The selectivity of probes was monitored by screening other anions such as F^-, Cl^-, Br^-, I^-, AcO^-, HSO_4^-, SCN^-, NO_3^-, and ClO_4^-. Color changes were not observed for probes in the presence of the other anions. In addition, Probes 1-4 containing electron-donating substituents showed faster detection compared to probes 5,6 containing electron-withdrawing substituents, proving that the sensitivity can be controlled.

Keywords

CN^- ion Sensor, water-soluble, Colorimetric chemosensor, selectivity

Introduction

Anions play vital roles in many areas such as biological applications, environmental issues, catalysis, and clinical compounds.[1,2] Among various anion targets, cyanide is one of the most useful anions that is widely utilized in many fields.[3–5] Nevertheless, cyanide anion (CN^-) is highly toxic to the human body.[6] Strong binding of CN^- ion to a heme unit of cytochrome *c* paralyzes cellular respiration[7] and causes severe damage to the central nervous system.[8] However, cyanides are versatile reagents in industry for synthesis[9] and metallurgy,[10] inevitably leading to accidental release of CN^- into the environment. The maximum permissive level of cyanide in drinking water is 1.9 μM according to the World Health Organization (WHO).[11] Therefore, an accurate level of quantification of CN^- ion is highly necessary for environmental samples.

Numerous analytical methods such as voltammetry, potentiometry, and chromatography have been used for CN^- ion detection[12-14]; although they successfully detect very low levels of CN^- (<0.1 μM), these methods require tedious sample pretreatment or expensive instrumentation. Therefore, selective and sensitive detection of cyanide ion has recently attracted considerable interest in the fields of environmental protection and human healthcare.[15-17] To date, a variety of cyanide sensors have been developed based on different mechanisms, such as supramolecular self-assembly,[18] nucleophilic addition,[19-30] hydrogen bonding motifs,[31-35] cyanide complexation addition,[36] electron deficient alkenes,[37] and other schemes.[38-41] However, most of these sensors are not soluble in aqueous solution, and there are some limitations concerning method sensitivity and selectivity. Therefore, progress in this area requires new strategies for the selective recognition of CN^- with high selectivity, sensitivity, and naked eye detection in aqueous solution.

Herein, Design and synthesis of six derivatives of a conjugated hemicyanine-based probe are reported as cyanide sensors with significant dual colorimetric and % transmission properties. As the methylindocyanine C=N is an effective target for nucleophilic analytes, cyanide easily reacts with this moiety, inducing remarkable change in spectroscopic properties. With the gradual addition of cyanide, the initially colored solutions changed to colorless, which offers the possibility for detection of cyanide by the “naked eye.” Other anions such as F^-, Cl^-, Br^-, I^-, AcO^-, HSO_4^-, SCN^-, NO_3^-, and ClO_4^- did not cause any significant interference with the hemicyanine chromophore.

Experimental

All chemicals and reagents were purchased from commercial sources, and the solvents used were of spectroscopic grade. ^{1}H nuclear magnetic resonance (NMR) spectra of compounds were collected in DMSO-d_6 on a Bruker Advance 300 MHz NMR spectrometer. UV–vis and PL spectra were recorded on Varian Cary 100 and HORIBA FluoroMax-4Pm spectrophotometers, respectively.

Synthesis of Chemosensors

Synthesis of probe 1. To prepare probe 1, 3.32 mmol (1.0 g) of 1,2,3,3-tetramethyl-3H-indolium iodide dissolved in 20 mL of ethanol was treated with 0.5425 g (3.9844 mol) of 4-methoxybenzaldehyde in the presence of piperidine (catalytic amount) and stirred at 65 °C for 24 h. After cooling to room temperature, the precipitate was washed with 30 mL of methanol, collected by filtration, and dried at 40 °C for 16 h to obtain a colored solid.

^{1}H NMR (300 MHz, $CDCl_3$), δ (ppm): 8.38 (1H, d), 8.22 (2H, d), 7.86 (2H, d), 7.59-7.65 (2H, broad), 7.53 (1H, d), 7.15 (2H, d), 4.11 (3H, s), 3.90 (3H, s), 1.78 (6H, s). UV-vis (H_2O, 5.0×10^{-6} mol L^{-1}): max (nm): 406.

Probe 1 + CN^-. ^{1}H NMR (300 MHz, $CDCl_3$), δ (ppm): 7.58 (2H, d), 7.15-7.19 (2H, multiplet), 6.91-6.97 (3H, multiplet), 6.85 (1H, t), 6.72 (1H, d), 6.27 (1H, d), 3.77 (3H, s), 2.71 (3H, s), 1.46 (3H, s), 1.11 (3H, s).

Synthesis of probe 2. For this preparation, 0.4228 g (3.9844 mol) of benzaldehyde was used in an analogous procedure to that used for probe 1.

^{1}H NMR (300 MHz, $CDCl_3$), δ (ppm): 8.40 (1H, d), 8.23 (1H, broad s), 8.20 (1H, d), 7.88-7.94 (2H, multiplet), 7.69 (H, d), 7.57-7.66 (5H, multiplet), 4.17 (3H, s), 1.80 (6H, s). UV-vis (H_2O, 5.0×10^{-6} mol L^{-1}): max (nm): 378.

Probe 2 + CN^-. ^{1}H NMR (300 MHz, $CDCl_3$), δ (ppm): 7.64 (2H, d), 7.35-7.43 (3H, multiplet), 7.15-7.20 (2H, multiplet), 6.98 (1H, d), 6.85 (1H, t), 6.73 (1H, d), 6.45 (1H, d), 2.73 (3H, s), 1.48 (3H, s), 1.12 (3H, s).

Synthesis of probe 3. Here, 0.5265 g (3.9844 mol) of 3-vinylbenzaldehyde was used in an analogous procedure to that used for probe 1.

^{1}H NMR (300 MHz, $CDCl_3$), δ (ppm): 8.40 (1H, d), 8.31 (1H, s), 8.13 (1H, d), 7.89-7.95 (2H, multiplet), 7.74 (H, d), 7.71 (H, s), 7.63-7.66 (2H, multiplet), 7.58 (H, t), 6.79-6.88 (H, dd), 6.02 (H, s), 5.42 (H, s), 4.18 (3H, s), 1.80 (6H, s). UV-vis (H_2O, 5.0×10^{-6} mol L^{-1}): max (nm): 379.

Probe 3 + CN^-. ^{1}H NMR (300 MHz, $CDCl_3$), δ (ppm): 7.78 (H, d), 7.55 (1H, s), 7.44 (1H, s), 7.37 (H, t), 7.15-7.20 (2H, multiplet), 6.98 (1H, d), 6.81-6.88 (1H, dd), 6.71-6.77 (2H, multiplet), 6.51 (1H, d), 5.93 (1H, d), 5.29 (1H, d), 2.73 (3H, s), 1.48 (3H, s), 1.12 (3H, s).

Synthesis of probe 4. Probe 4 was prepared using 0.4787 g (3.9844 mol) of 4-methylbenzaldehyde in an analogous procedure to that used for probe 1.

^{1}H NMR (300 MHz, $CDCl_3$), δ (ppm): 8.37 (1H, d), 8.12 (2H, d), 7.87-7.92 (2H, multiplet), 7.59-7.69 (3H, multiplet), 7.41 (2H, d), 4.14 (3H, s), 2.42 (3H, s), 1.79 (6H, s). UV-vis (H_2O, 5.0×10^{-6} mol L^{-1}): max (nm): 392.

Probe 4 + CN^-. ^{1}H NMR (300 MHz, $CDCl_3$), δ (ppm): 7.51 (2H, d), 7.14-7.22 (4H, multiplet), 6.92 (1H, d), 6.84 (1H, t), 6.72 (1H, d), 6.36 (1H, d), 2.71 (3H, s), 2.31 (3H, s), 1.46 (3H, s), 1.10 (3H, s).

Synthesis of probe 5. In an analogous procedure to that used for probe 1, 0.6470 g (3.6524 mol) of 4-nitrobenzaldehyde was used to prepared probe 5.

^{1}H NMR (300 MHz, $CDCl_3$), δ (ppm): 8.50 (1H, d), 8.46 (2H, d), 8.40 (2H, d), 7.86-8.00 (3H, multiplet), 7.65-7.77 (2H, multiplet), 4.32 (3H, s), 1.81 (6H, s). UV-vis (H_2O, 5.0×10^{-6} mol L^{-1}): max (nm): 377.

Probe 5 + CN^-. ^{1}H NMR (300 MHz, $CDCl_3$), δ (ppm): 8.22 (2H, d), 7.96 (2H, d), 7.13-7.20 (3H, multiplet), 6.75-6.88 (3H, multiplet), 2.74 (3H, s), 1.50 (3H, s), 1.12 (3H, s).

Synthesis of probe 6. For synthesis of probe 6, 0.6359 g (3.6524 mol) of 4-(trifluoromethyl)benzaldehyde was used in an analogous procedure to that used for probe 1.

^{1}H NMR (300 MHz, $CDCl_3$), δ (ppm): 8.41-8.49 (3H, multiplet), 7.96-7.98 (3H, multiplet), 7.90-7.93 (1H, dd), 7.82 (1H, d), 7.64-7.70 (2H, multiplet), 4.21 (3H, s), 1.81 (6H, s). UV-vis (H_2O, 5.0×10^{-6} mol L^{-1}): max (nm): 369.

Probe 6 + CN^-. ^1H NMR (300 MHz, $CDCl_3$), δ (ppm): 7.89 (2H, d), 7.66-7.76 (2H, t), 7.13-7.21 (2H, multiplet), 7.08 (1H, d), 6.86 (1H, t), 6.74 (1H, d), 6.64 (1H, d), 2.74 (3H, s), 1.49 (3H, s), 1.12 (3H, s).

Preparation of probe stock solutions

Stock solution for each probe was prepared at a concentration of 1.0×10^{-3} mL^{-1} in 10 mL of H_2O. The stock solution was diluted with aqueous solution to the desired concentration for each titration in a 0.5 mL cuvette.

Preparation of anion stock solutions

Each anion stock solution was prepared at a concentration of 10×10^{-3} mL^{-1} in 10 mL of distilled water. Stock solutions were diluted to the desired concentrations with distilled water as needed.

UV−visible study of probes with cyanide ion

The UV−vis spectra of probes 1-6 were recorded in water (100%) using 40.0 μM concentrations of probes. Probes 1-6 showed maximum absorption bands at 406, 378, 379, 392, 377, and 369 nm, respectively. Further, the absorbance of probes 1-6 decreased linearly with increasing addition of CN^- ions (5.0 or 10 equiv.) in water.

Results and discussion

As a member of the cyanine dye family,[42] hemicyanines have applications in many research fields such as dye-sensitized solar cells[43,44] and in biological applications.[45] Hemicyanines have been used as chemosensors due to their unique structural photophysical properties including good biocompatibility and low cytotoxicity. In particular, the structural system of the hemicyanine chemosensor is designed as donor–π–acceptor (D–π–A) in which a positively charged nitrogen heterocyclic moiety as electron acceptor and a terminal alkyl, hydroxyl, alkoxy, or amino group as electron donor are connected through a conjugated aromatic system. Generally, the synthesis of hemicyanine-based chemosensors involves condensation of heterocyclic bases containing activated methyl groups with benzaldehyde derivatives.[46] Typically, hemicyanines display large Stokes shifts due to the strong excited-state intramolecular charge transfer (ICT) process from electron donor to acceptor moiety. The combined synergistic photophysical properties of hemicyanine allow it to be used as an effective new platform for the design of chemosensors. The detection of target analytes utilizing hemicyanine-based chemosensors is usually realized by adjusting the ICT process (ICT enhancement or ICT blocking) of the electron donor. Therefore, in this study, Six different chemosensors were developed by modulating the electron-donating ability of the donors in order to obtain absorption wavelength shifts for colorimetric or ratiometric mode sensors.

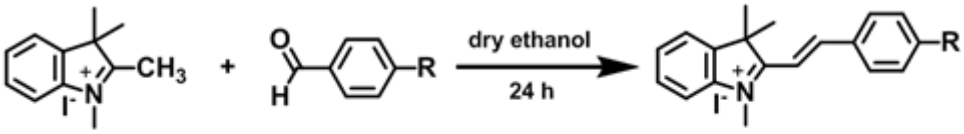

Probe 1: R = OCH_3; Probe 2: R = H; Probe 3: R = 3-vinyl
Probe 4: R = CH_3; Probe 5: R = NO_2; Probe 6: R = CF_3

Scheme 1. Synthesis schemes of Probes 1-6.

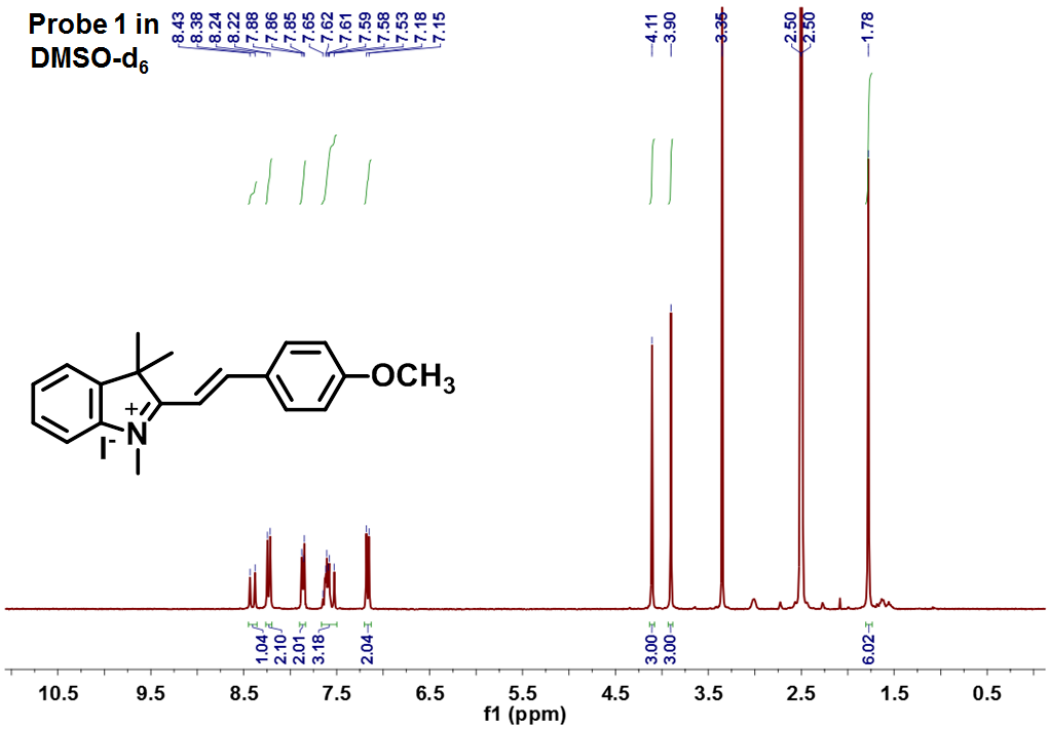

Figure 1. ^{1}H NMR spectra of Probe 1 in DMSO-d_6.

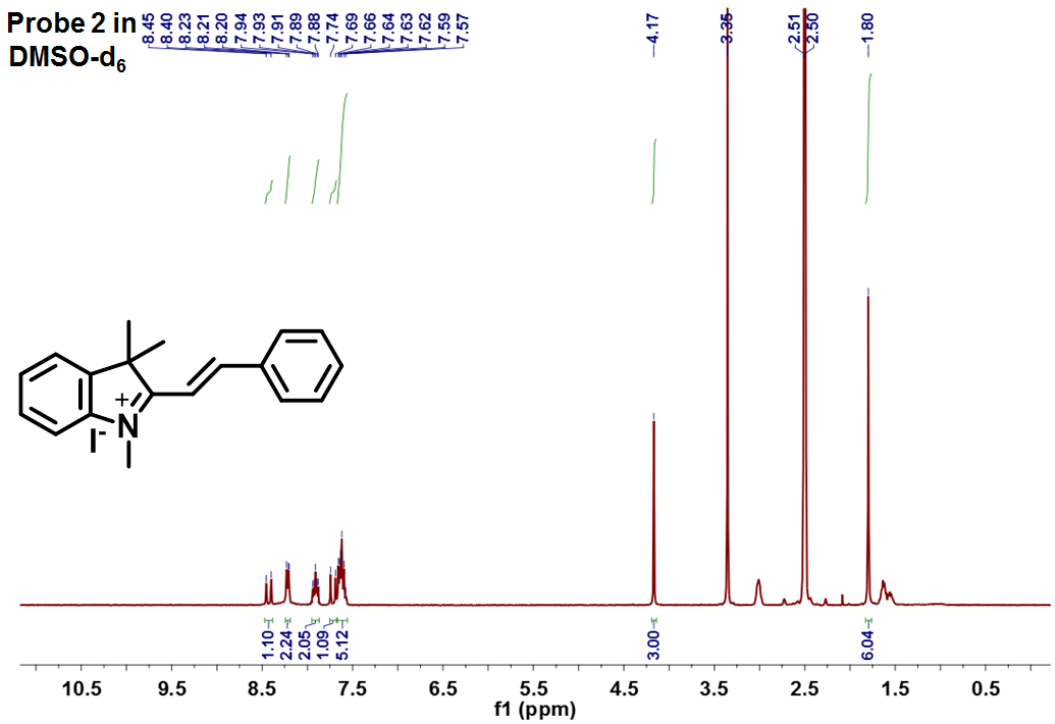

Figure 2. ^{1}H NMR spectra of Probe 2 in DMSO-d_6.

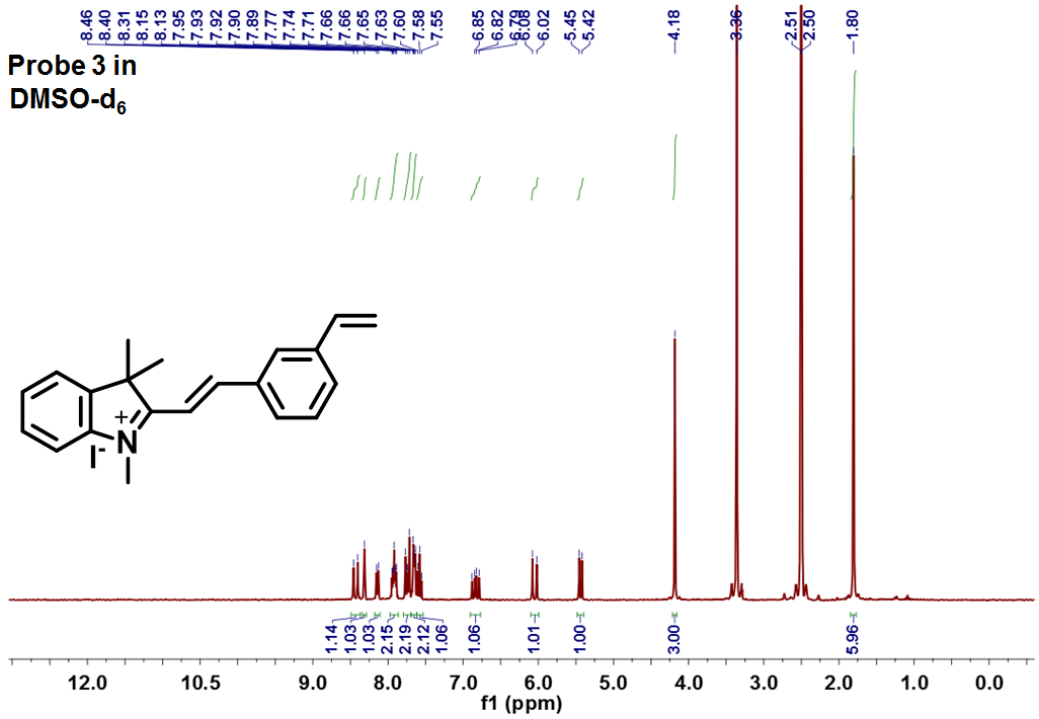

Figure 3. ^{1}H NMR spectra of Probe 3 in DMSO-d_6.

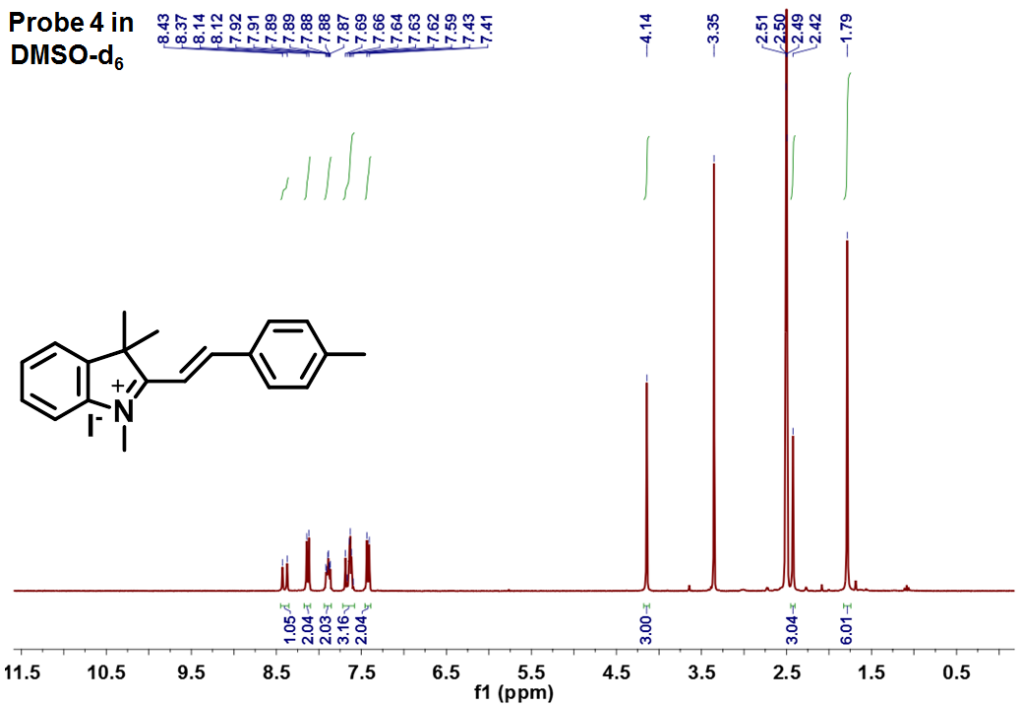

Figure 4. ^{1}H NMR spectra of Probe 4 in DMSO-d_6.

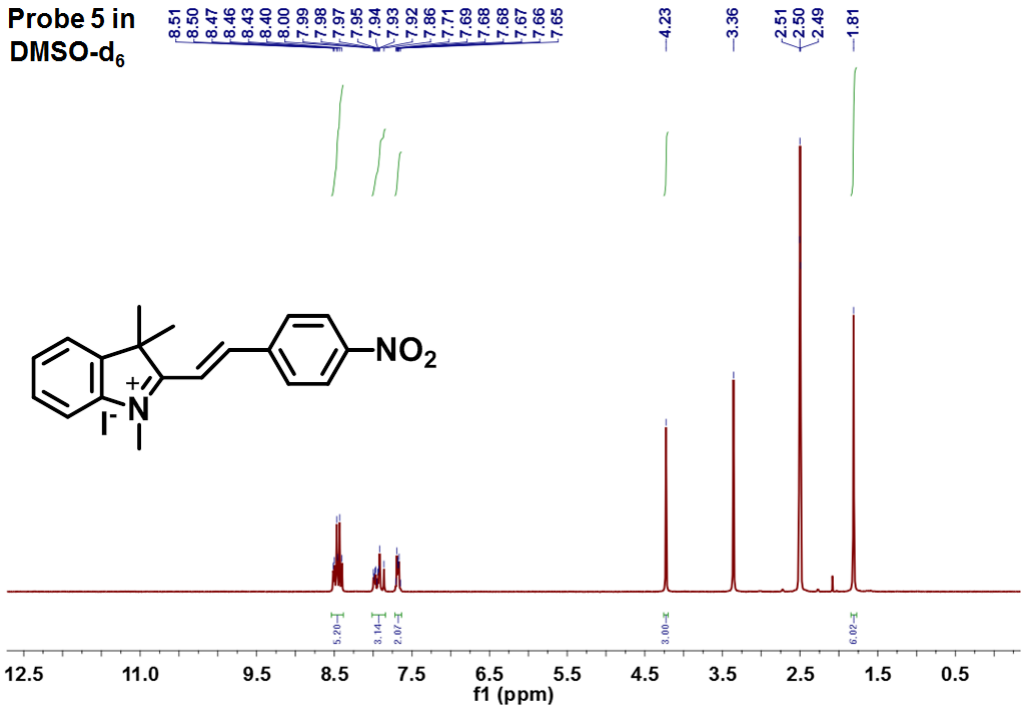

Figure 5. ^{1}H NMR spectra of Probe 5 in DMSO-d$_6$.

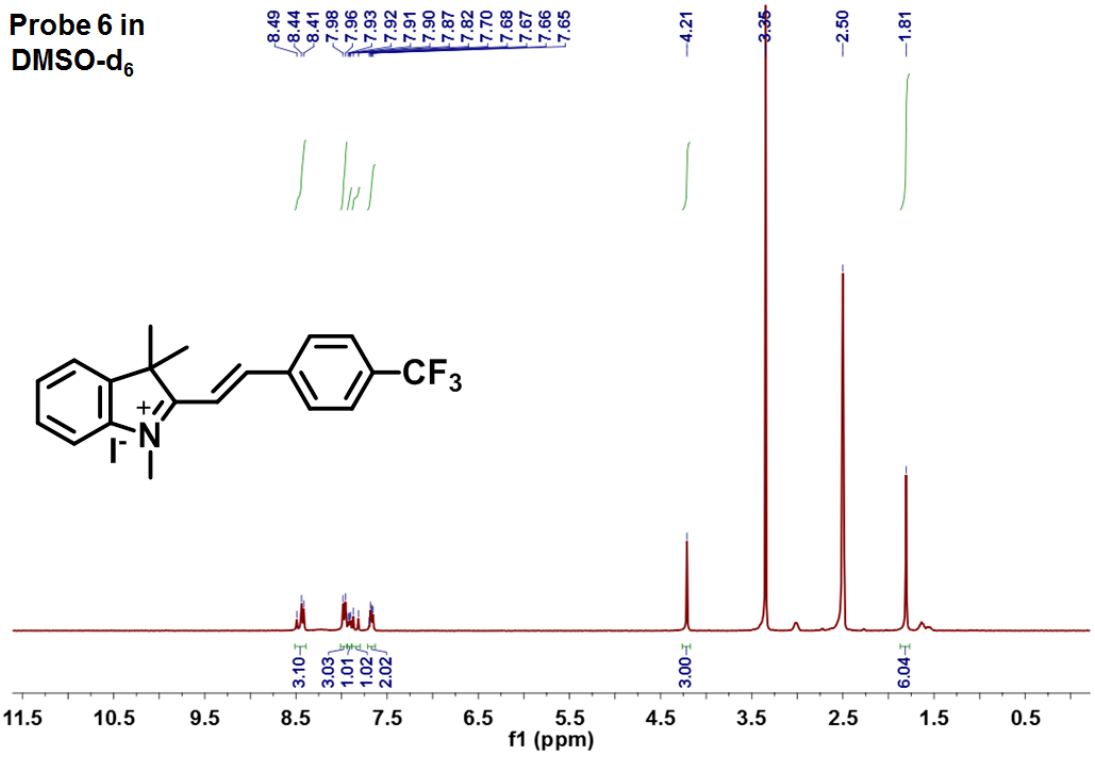

Figure 6. ^{1}H NMR spectra of Probe 6 in DMSO-d$_6$.

Through condensation reactions of 1,2,3,3-tetramethyl-3H-indol-1-ium iodide, six different benzaldehyde derivatives were appended through a C=C double bond to give hemicyanine derivatives containing electron-donating or electron-withdrawing functional groups (Scheme 1). The resulting molecules were characterized using ^{1}H NMR spectroscopy (Figure 1-6). The indolium group has a strong electron-withdrawing effect because of the positively charged nitrogen atom to provide an effective electron acceptor. As shown in Scheme 1, OCH_3, H, 3-vinyl, CH_3, NO_2, and CF_3 groups were linked via benzaldehyde to give six different electron-rich or electron-deficient conjugated donors. Due to this linking reaction, intramolecular charge transfer (ICT) was expected to occur from the donors to the indolium acceptor. Furthermore, cyanide addition to the $C=N^+$ electrophilic double bond was expected to reduce the electron-withdrawing effect of the indolium group and to disturb the ICT process through conversion and neutralization of the $C=N^+$ double bond, with concomitant appearance of corresponding optical changes.

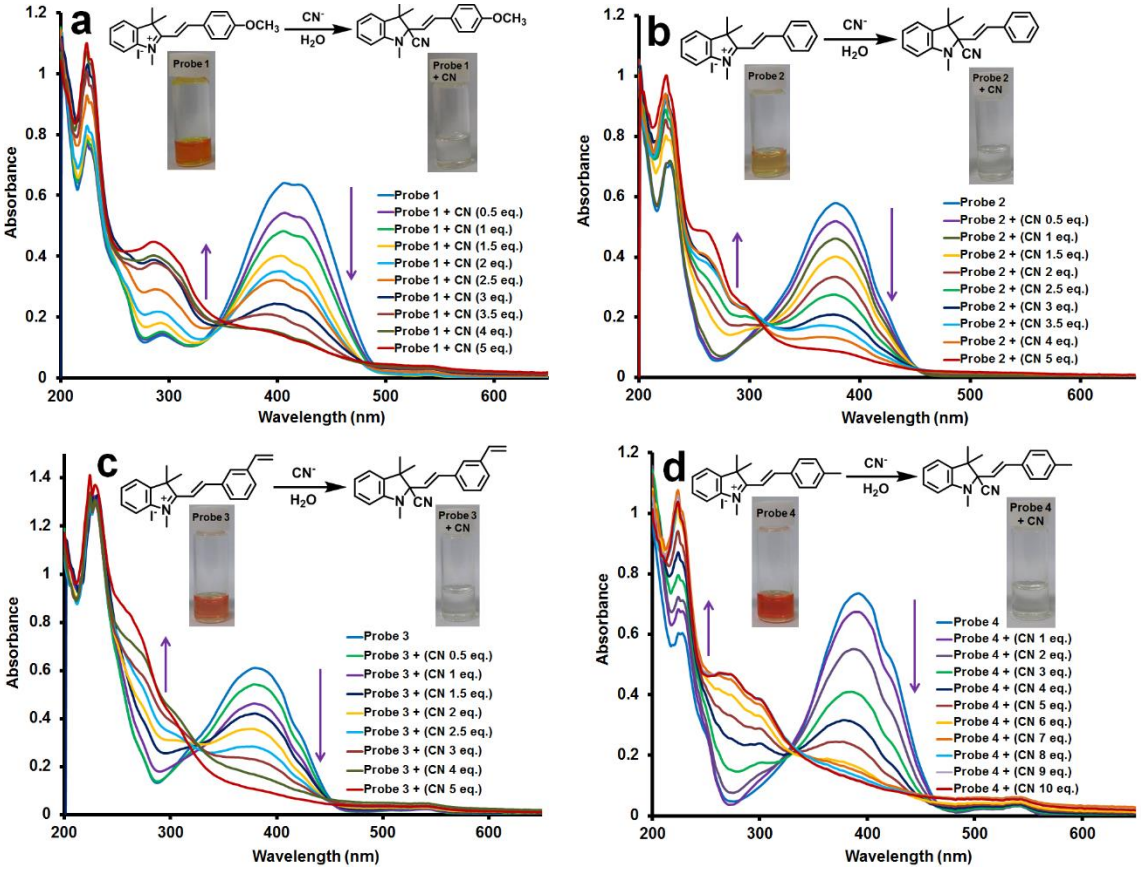

Figure 7. (a-c) Changes in absorption spectra of probes 1, 2, and 3 (40 μM) measured in 100% water solution upon addition of CN^- (5.0 equiv.); (d) Changes in absorption spectra of probe 4 (40 μM) measured in 100% water solution upon addition of CN^- (1-10.0 equiv.).

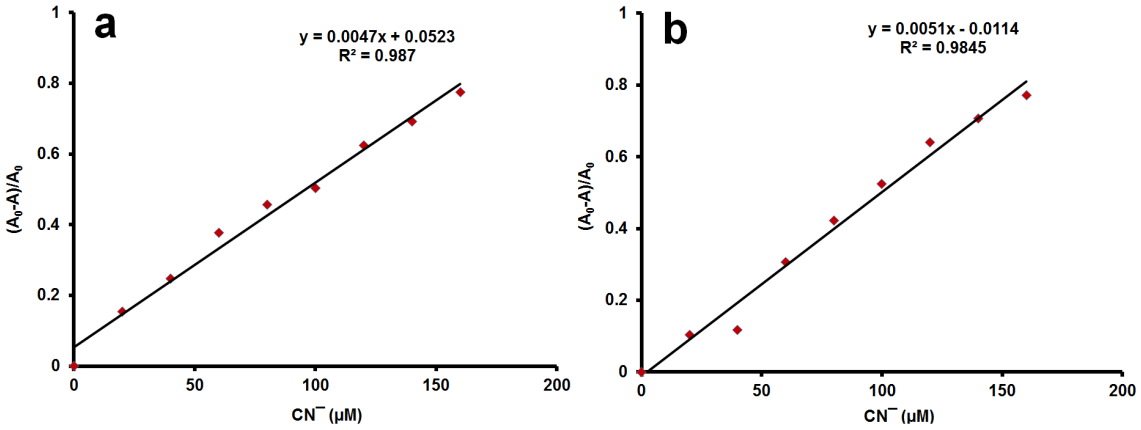

Figure 8. (a) Absorption spectra of linear fitted plot for probe 1 at 406 nm change against cyanide concentration (20-160 μM); (b) Absorption titration spectra of linear fitted plot for probe 2 at 378 nm change against cyanide concentration (20-160 μM).

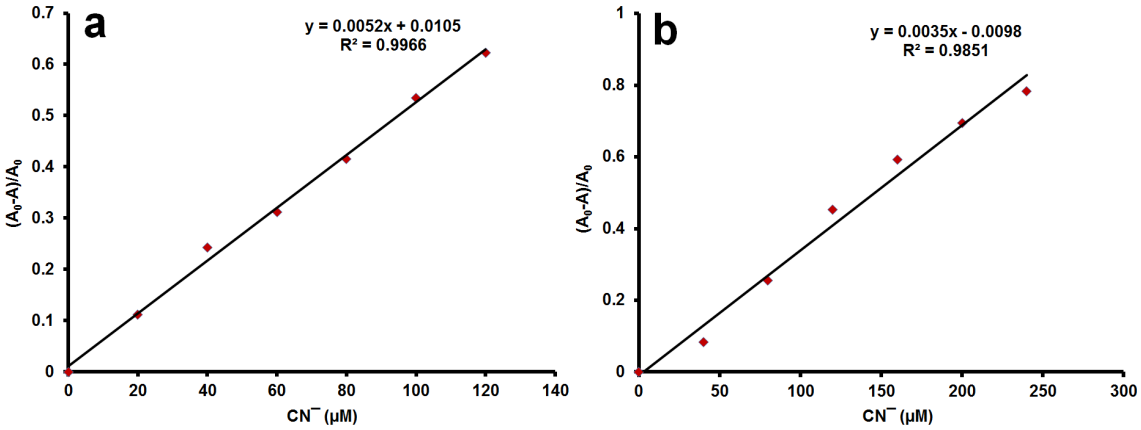

Figure 9. (a) Absorption spectra of linear fitted plot for probe 3 at 379 nm change against cyanide concentration (20-120 μM); (b) Absorption titration spectra of linear fitted plot for probe 4 at 392 nm change against cyanide concentration (20-240 μM).

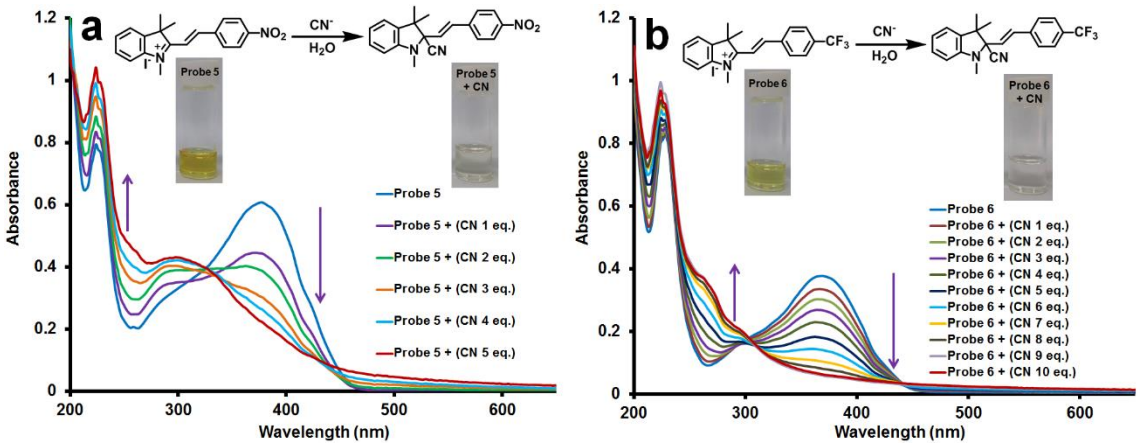

Figure 10. (a) Changes in absorption spectra of probe 5 (40 μM) measured in 100% water solution upon addition of CN^- (5 equiv.). (b) Changes in absorption spectra of and 6 (40 μM) measured in 100% water solution upon addition of CN^- (1-10.0 equiv.).

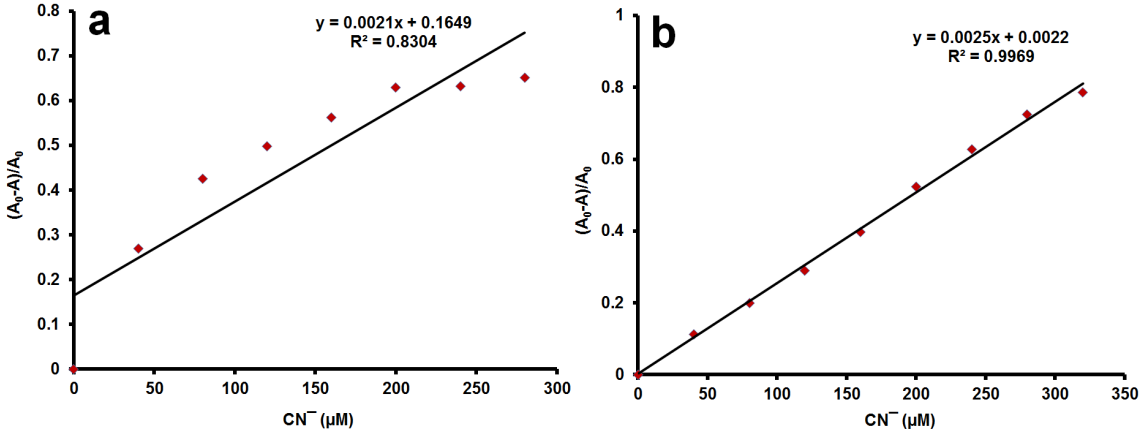

Figure 11. (a) Absorption spectra of linear fitted plot for probe 5 at 377 nm change against cyanide concentration (20-280 μM); (b) Absorption titration spectra of linear fitted plot for probe 6 at 369 nm change against cyanide concentration (20-320 μM).

Changes in the absorption spectra of probes 1 and 2 upon titration with CN^- in 100% water were recorded (Fig. 7). As shown in Fig. 7a, probe 1 exhibited a main absorption peak at 406 nm, which was ascribed to the typical intramolecular charge transfer (ICT) band of hemicyanine chromophores. Upon addition of CN^-, the absorbance gradually decreased, with a new peak appearing at 286 nm, until saturation was reached after titration with 5.0 equiv. of CN^-. Simultaneously, an obvious color change from an initial orange solution to colorless was clearly observed, suggesting that the ICT was turned off due to nucleophilic attack of CN^- at the indolium group of probe 1. Moreover, a plot of $(A_0\text{-}A/A_0)$, where A_0 and A were the respective absorbances at 406 nm in the absence and presence of CN^-, vs. concentration was found to be almost linear when the concentration of CN^- was in the range of 20-160 μM (Fig. 8a). The limit of detection calculated for CN^- based on 3σ/slope was 0.36 μM, which is a considerably lower concentration compared to the level of cyanide permitted in drinking water according to the WHO.[47]

Similarly, increasing concentrations of CN^- with probe 2 led to a gradual decrease in absorbance at 378 nm and a new peak appearing at 254 nm until saturation was reached after titration with 5.0 equiv. of CN^-. Simultaneously, an obvious color change from an initial yellow solution to colorless was clearly observed, suggesting that ICT was turned off due to nucleophilic attack of CN^- on the indolium group of probe 2. Moreover, a plot of $(A_0\text{-}A/A_0)$, where A_0 and A were the respective absorbances at 378 nm in the absence and presence of CN^-, vs. concentration was found to be almost linear when the concentration of CN^- was in the range of 20-160 μM (Fig. 8b). The limit of detection calculated for CN^- based on 3σ/slope was 2.93 μM.[47]

As shown in Fig. 7, probe 3 exhibited a main absorption peak at 379 nm, which was ascribed to the typical intramolecular charge transfer (ICT) band of hemicyanine chromophores. Upon addition of CN^-, the absorbance gradually decreased, with a new peak or shoulder appearing at 252 nm until saturation was reached after titration with 5.0 equiv. of CN^-. Simultaneously, an obvious color change from the initial reddish orange solution to colorless was clearly observed. Moreover, a plot of $(A_0\text{-}A/A_0)$, where A_0 and A were the respective absorbances at 379 nm in the absence and presence of CN^-, vs. concentration was found to be almost linear when the concentration of CN^- was in the range of 20-120 μM (Fig. 9a). The limit of detection calculated for CN^- based on 3σ/slope was 3.34 μM.[47]

Similarly, increasing concentrations of CN^- with probe 4 led to a gradual decrease in

absorbance at 392 nm and a new peak appearing at 263 nm until saturation was reached after titration with 5.0 equiv. of CN^-. Simultaneously, an obvious color change from the initial yellow solution to colorless was clearly observed. Moreover, a plot of (A_0-A/A_0), where A_0 and A were the respective absorbances at 392 nm in the absence and presence of CN^-, vs. concentration was found to be almost linear when the concentration of CN^- was in the range of 20-240 μM (Fig. 9b). The detection limit calculated for CN^- based on 3σ/slope was 3.94 μM.[47] As shown in Fig. 10, probe 5 exhibited a main absorption peak at 377 nm, which was ascribed to the typical intramolecular charge transfer (ICT) band of hemicyanine chromophores. Upon addition of CN^-, the absorbance gradually decreased, with a new peak appearing at 299 nm until saturation was reached after titration with 5.0 equiv. of CN^-. Simultaneously, an obvious color change from the initial greenish yellow solution to colorless was clearly observed. A plot of (A_0-A/A_0), where A_0 and A were the respective absorbances at 377 nm in the absence and presence of CN^-, vs. concentration was found to be almost linear when the concentration of CN^- was in the range of 20-280 μM (Fig. 11a).

Similarly, increasing concentrations of CN^- with probe 6 led to gradually decreasing absorbance at 369 nm and a new peak or shoulder appearing at 258 nm until saturation was reached after titration with 5.0 equiv. of CN^-. Simultaneously, an obvious color change from the initial greenish yellow solution to colorless was clearly observed. A plot of (A_0-A/A_0), where A_0 and A were the respective absorbances at 369 nm in the absence and presence of CN^-, vs. concentration was found to be almost linear when the concentration of CN^- was in the range of 20-320 μM (Fig. 11b). The limit of detection calculated for CN^- based on 3σ/slope was 8.36 μM.[47]

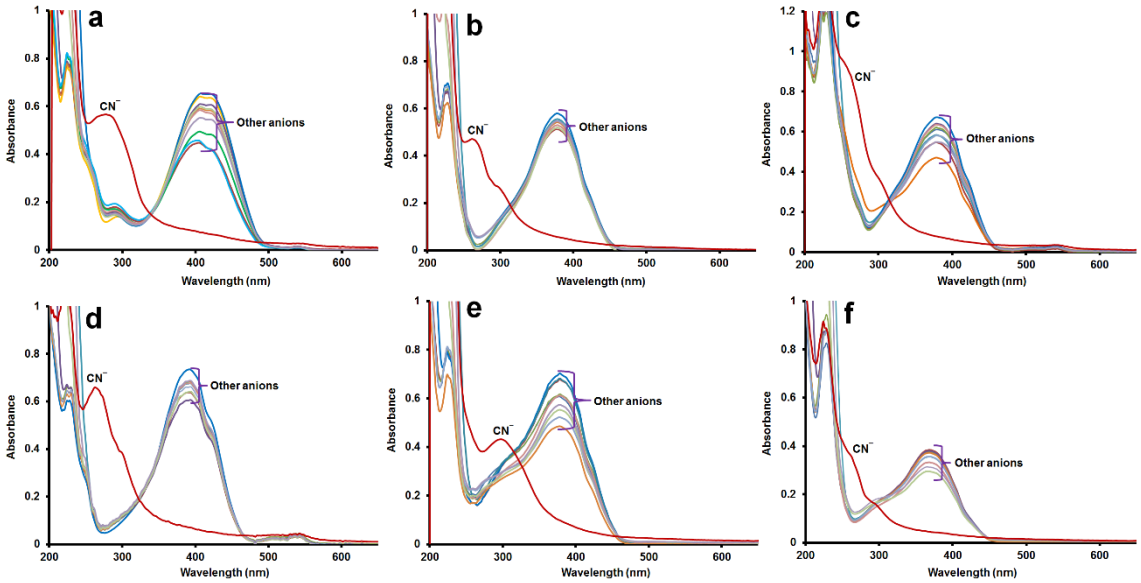

Figure 12. (a-d) UV–Visible spectra of probe 1-4 upon addition of CN^- (5 equiv.) in the presence of 5 equiv. of other competitive anions in 100% water; (e,f) UV–Visible spectra of probe 4-6 upon addition of CN^- (10 equiv.) in the presence of 5 equiv. of other competitive anions in 100% water.

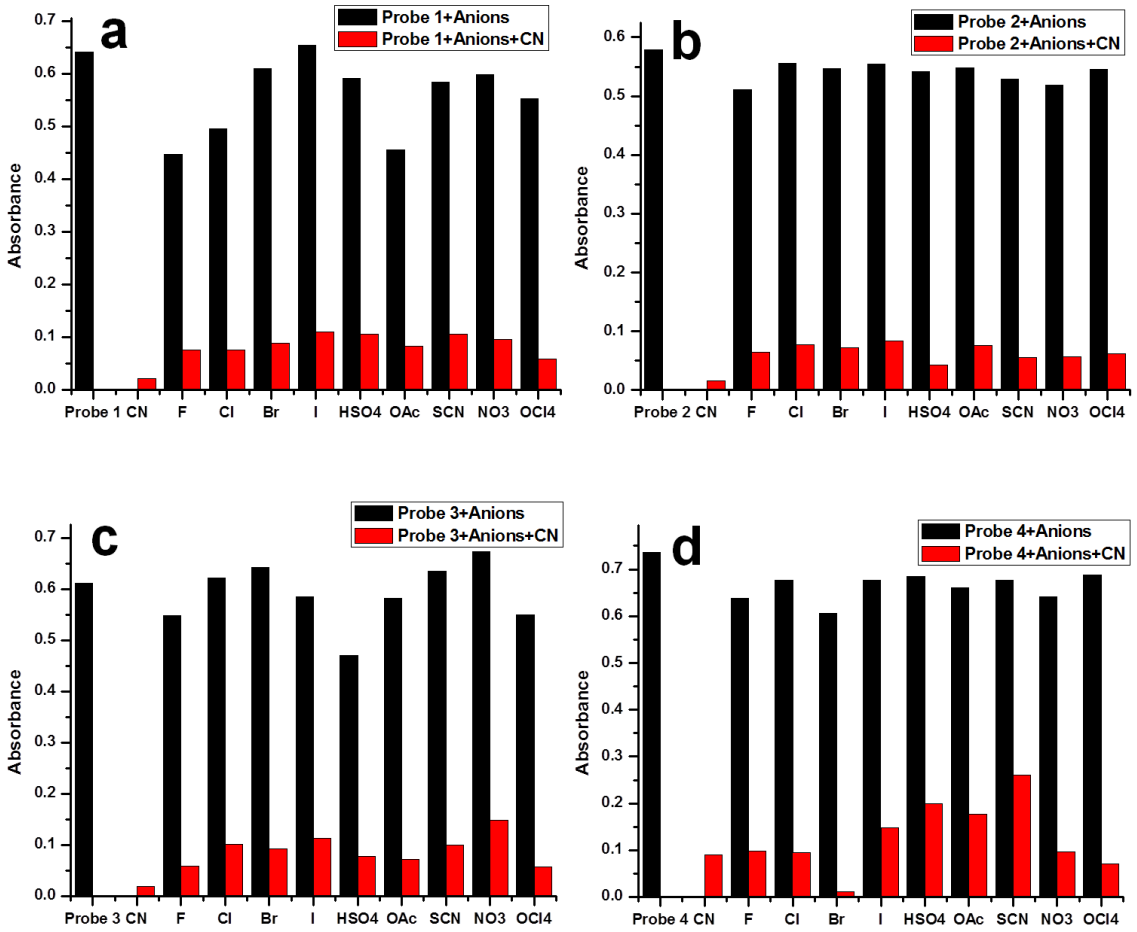

Figure 13. (a-d) UV–Visible spectra of probes 1-6 with addition of CN^- ion (5 equiv.) in the presence of 5 equiv. of competitive anions in 100% water.

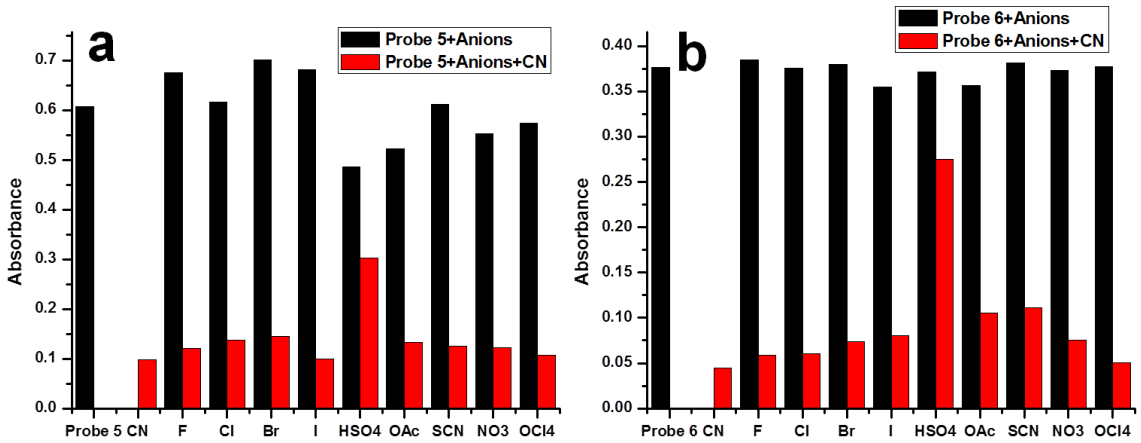

Figure 14. (a,b) UV–Visible spectra of probe 5 and 6 with addition of CN^- (10 equiv.) in the presence of 5 equiv. of other competitive anions in 100% water.

In order to study the special recognition ability of probes 1-6, competition experiments were analyzed by UV–vis spectrometry (Fig. 12). Figure 12 shows the absorbance changes of probes 1-6 upon addition of various analytes (5 equiv.) in 100% water including F^-, Cl^-, Br^-, I^-, AcO^-, HSO_4^-, SCN^-, NO_3^-, and ClO_4^-. All of these anions generated very minor changes with probes 1-6. However, the probes displayed dramatic UV–vis spectral changes in the presence of CN^- ion. As shown in Figs. 12(a-d), the absorption bands of probes 1-4 at 406, 378, 379, and 392 nm disappeared in the presence of CN^- ion (5 equiv.), and new blue-shifted absorption bands appeared at 286, 254, 252, and 263 nm due to intramolecular charge transfer (ICT) from the donors to the indolium acceptor. It is evident that the various competitive anions did not lead to any significant interference. Similarly, as shown in Figs. 12(e,f), the absorption bands of probes 5 and 6 at 377 and 369 nm disappeared in the presence of CN^- ion (10 equiv.), and new blue-shifted absorption bands appeared at 299 and 258 nm. In the presence of various competitive anions, CN^- ion still showed blue-shifted absorption changes. These signal changes indicate that the probes could serve as selective chemosensors for cyanide anions. In addition, selectivity assays were also performed in specially evaluated competitive experiments for probes 1-6 in the presence of CN^- ion and various anions in 100% water solution as described below (Fig. 13, 14).

To further evaluate the utility of probes 1-4 as anion selective sensors for CN^- ion, competitive experiments were carried out in the presence of 5 equiv. of CN^- together with various anions of F^-, Cl^-, Br^-, I^-, AcO^-, HSO_4^-, SCN^-, NO_3^-, and ClO_4^- in 100% water solution. As shown in the bar diagram (Figs. 13(a-d)), no significant interference was noticeable for probes 1-4 with the competitive anions. Similarly, competitive experiments were carried out for probes 5 and 6 in the presence of 10 equiv. of CN^- together with various anions in 100% water solution. As shown in the bar diagrams (Figs. 13(a,b)), no significant interference was noticeable for probes 5 and 6 with competitive anions. As can be seen in Figs. 14(a,b), only HSO_4^- showed slight interference with cyanide detection, but it did not lead to any significant absorbance changes, and the color of probes 5 and 6 remained almost unchanged. In the presence of various competitive species, the addition of CN^- resulted in similar absorbance changes.

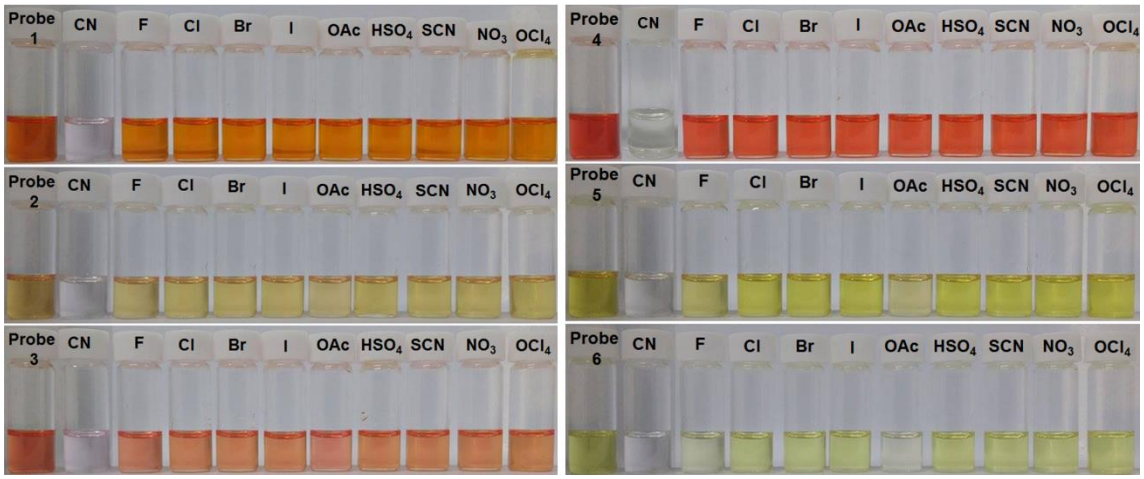

Figure 15. Colorimetric changes of probes 1-6 observed by the naked eye in the presence of 5 equiv. of various anions in aqueous solution (DMSO: H_2O; 9:1).

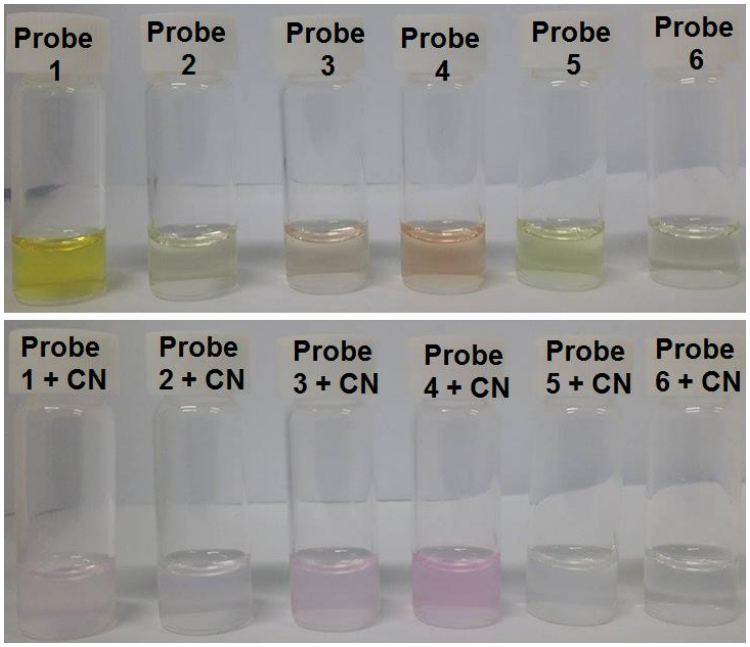

Figure 16. Colorimetric changes of probe 1-6 (100 μM) observed by naked eye in presence of 5 equiv. of various anions in 100% water.

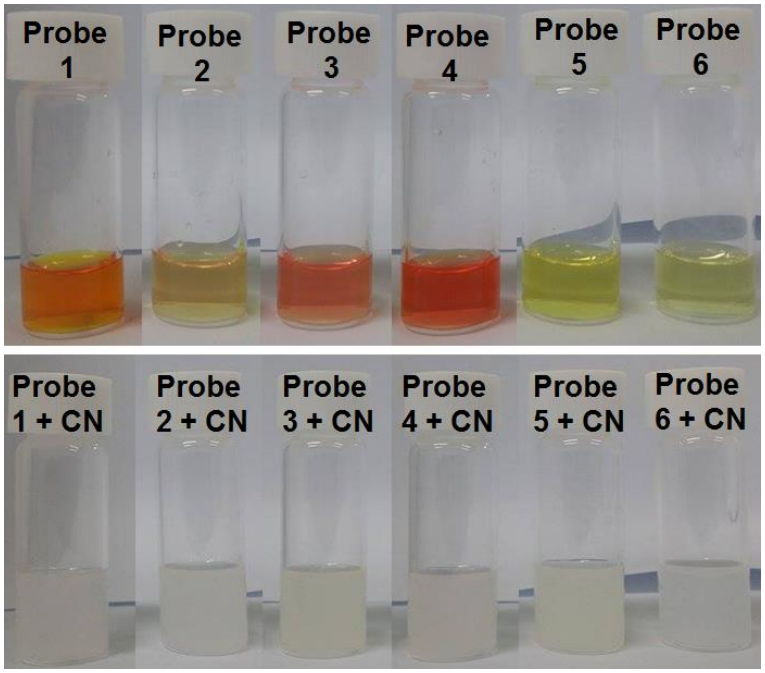

Figure 17. Colorimetric changes of probe 1-6 (1 mM) observed by naked eye in presence of 5 equiv. of various anions in 100% water.

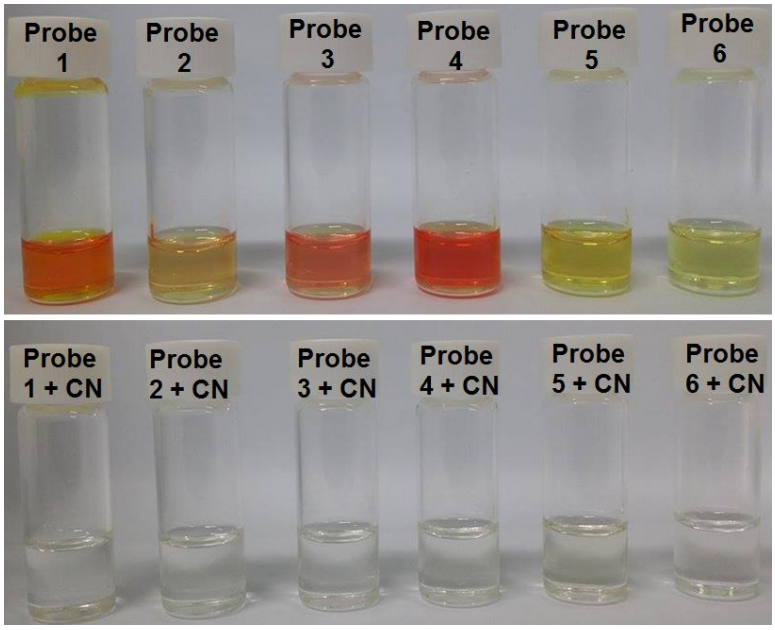

Figure 18. Colorimetric changes of probe 1-6 (1 mM) observed by naked eye in presence of 5 equiv. of various anions in aqueous solution (DMSO: H_2O; 9:1)

The colorimetric sensing ability of probes 1-6 was investigated by adding various anions such as CN^-, F^-, Cl^-, Br^-, I^-, AcO^-, HSO_4^-, SCN^-, NO_3^-, and ClO_4^- in aqueous solution (DMSO: H_2O; 9:1). Upon addition of CN^- ion (5 equiv.) to solutions of probes 1-6 at higher concentration (1 mM), probes 1-6 responded with a dramatic change from their respective colors to colorless solutions (Fig. 15). In contrast, upon addition of other anions of F^-, Cl^-, Br^-, I^-, AcO^-, HSO_4^-, SCN^-, NO_3^-, and ClO_4^- to the solutions of probes 1-6 (1 mM), no significant color changes were observed. Therefore, these probes could potentially be used as colorimetric probes for CN^- ion detection.

Moreover, the colorimetric sensing ability of probes 1-6 was investigated by adding CN^- ion in two different solvent systems, 100% water and aqueous DMSO solution (DMSO: H_2O; 9:1). Upon addition of CN^- ion (5 equiv.) to solutions of probes 1-6 at two different concentrations (100 μM and 1 mM), probes 1-6 responded slowly, with a color change from their respective colors to colorless solutions (Figs. 16, 17), due to the presence of turbidity. In contrast, upon addition of CN^- ion (5 equiv.) to solutions of probes 1-6 at higher concentration (1 mM) in aqueous solution (DMSO: H_2O; 9:1), probes 1-6 responded with dramatic color changes from the respective colors to colorless clear solutions (Fig. 18), and no turbidity was observed. Therefore, these probes could potentially be used as colorimetric probes for CN^- ion detection in aqueous solution (DMSO: H_2O; 9:1).

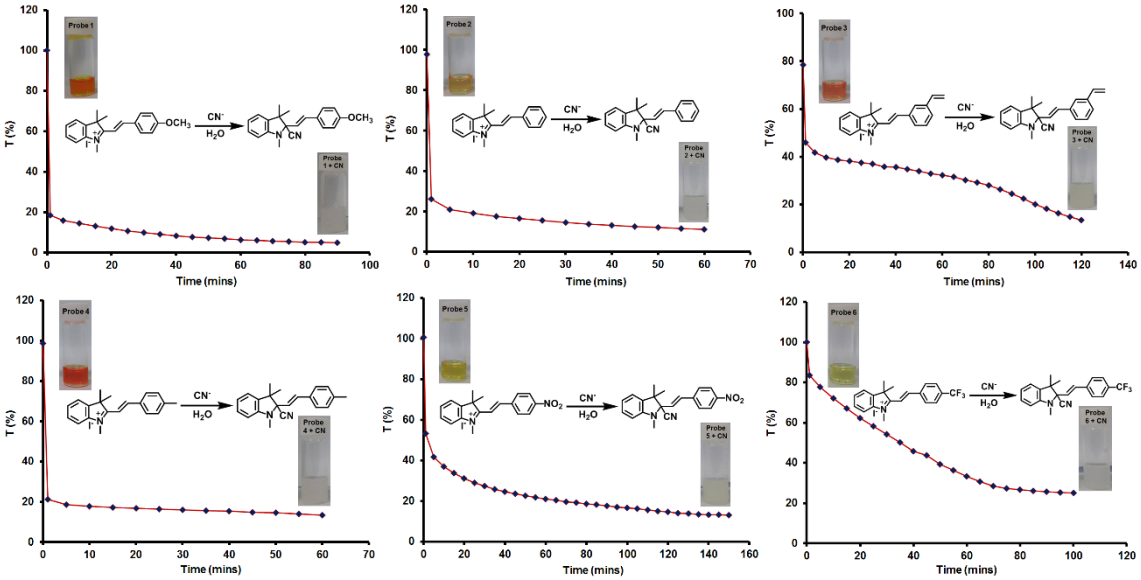

Figure 19. Time courses for reaction completion of probes 1-6 by monitoring transmittance changes at 620 nm in 100% water.

Due to these probes generating turbidity at higher concentrations in 100% water, the time course to reaction completion of probes 1-6 was examined by monitoring transmittance changes at 620 nm in 100% water (Figure 19). As shown in Figs. 19, reaction completion was monitored upon addition of CN^- ions (5 equiv.) to solutions of probes 1-6 and the reduction was observed in transmittance at 620 nm at different time intervals. As a result, probes 1-4 showed an immediate reduction in transmittance at 620 nm compared to probes 5 and 6, which indicates that electron-donating substituents (probes 1-4) induce faster reactions compared to electron-withdrawing groups (probes 5, 6). Moreover, this result strongly supports the reaction sensitivity of all of the probes, but probe 1 displaying unique sensitivity and selectivity for the detection of CN^- ions.

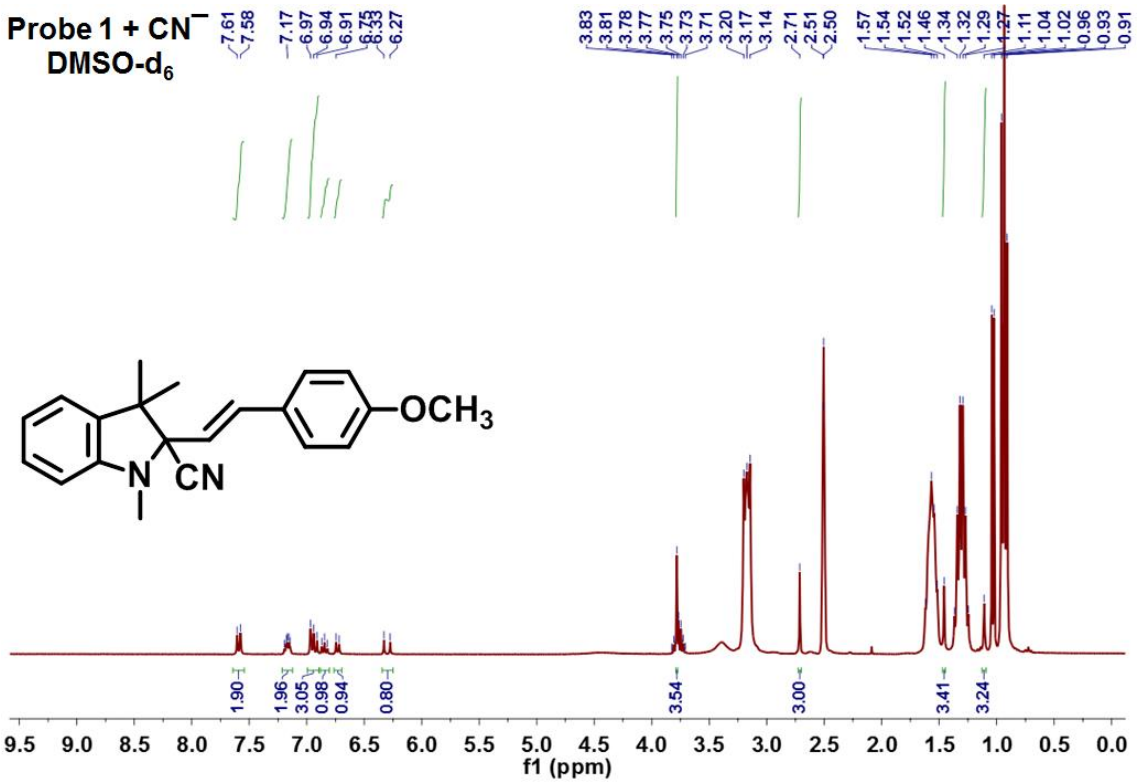

Figure 20. ^{1}H NMR spectra of Probe 1+ CN^{-} in DMSO-d_6.

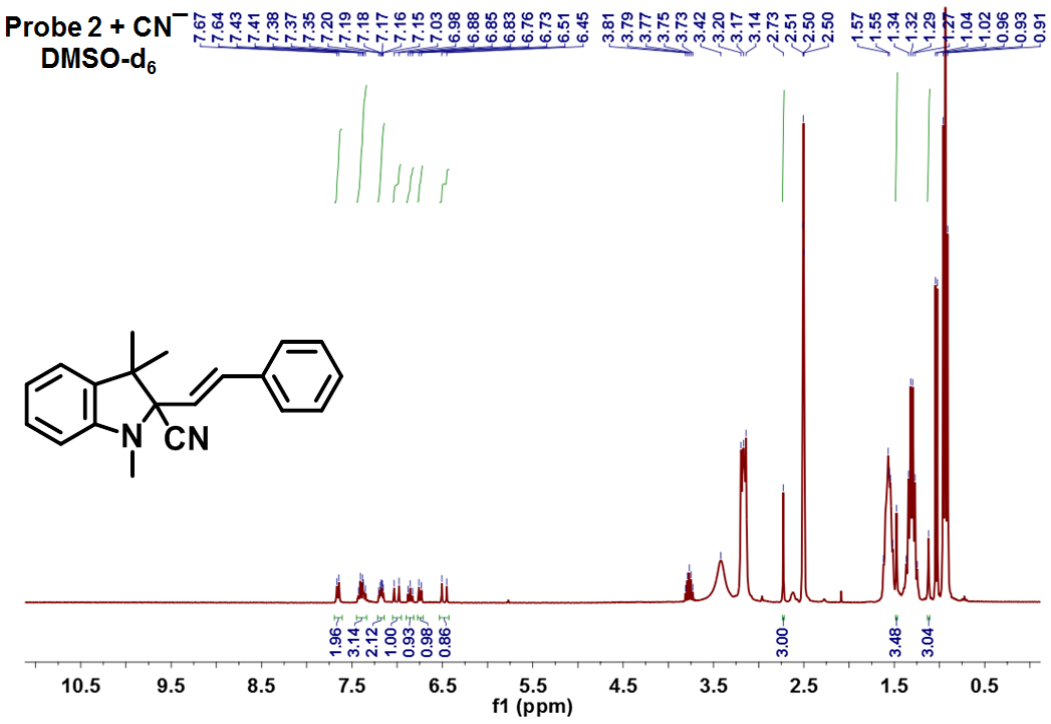

Figure 21. ^{1}H NMR spectra of Probe 2 + CN^{-} in DMSO-d_6.

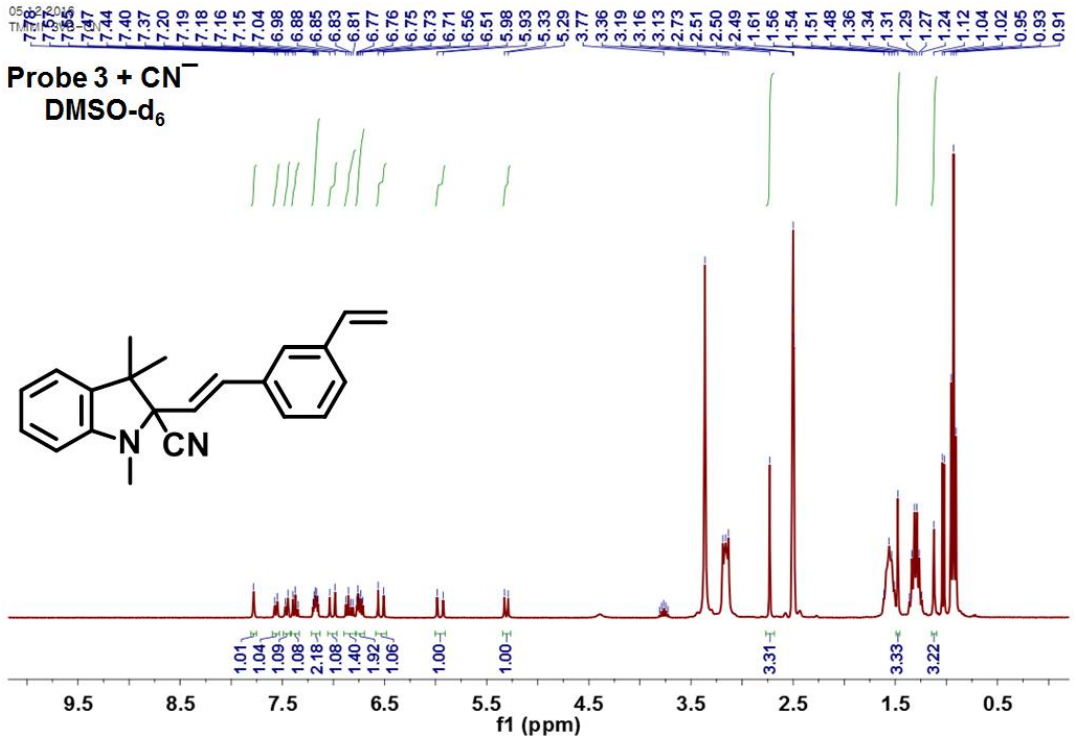

Figure 22. ^{1}H NMR spectra of Probe 3 + CN^{-} in DMSO-d_6.

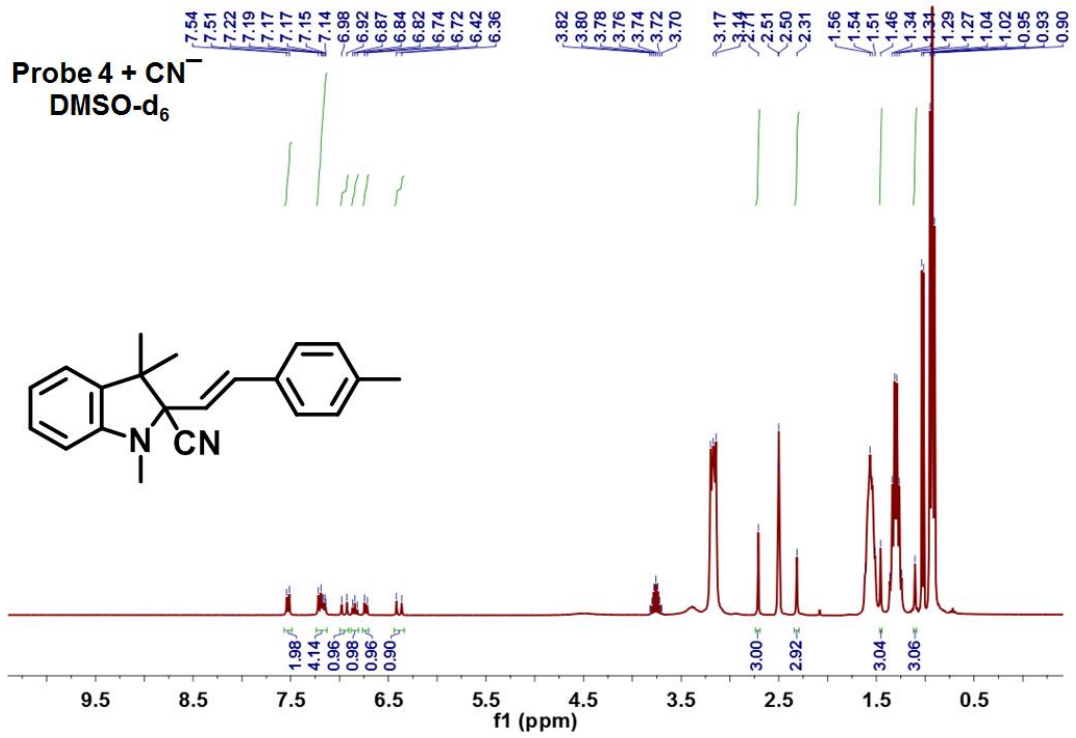

Figure 23. ^{1}H NMR spectra of Probe 4 + CN^{-} in DMSO-d_6.

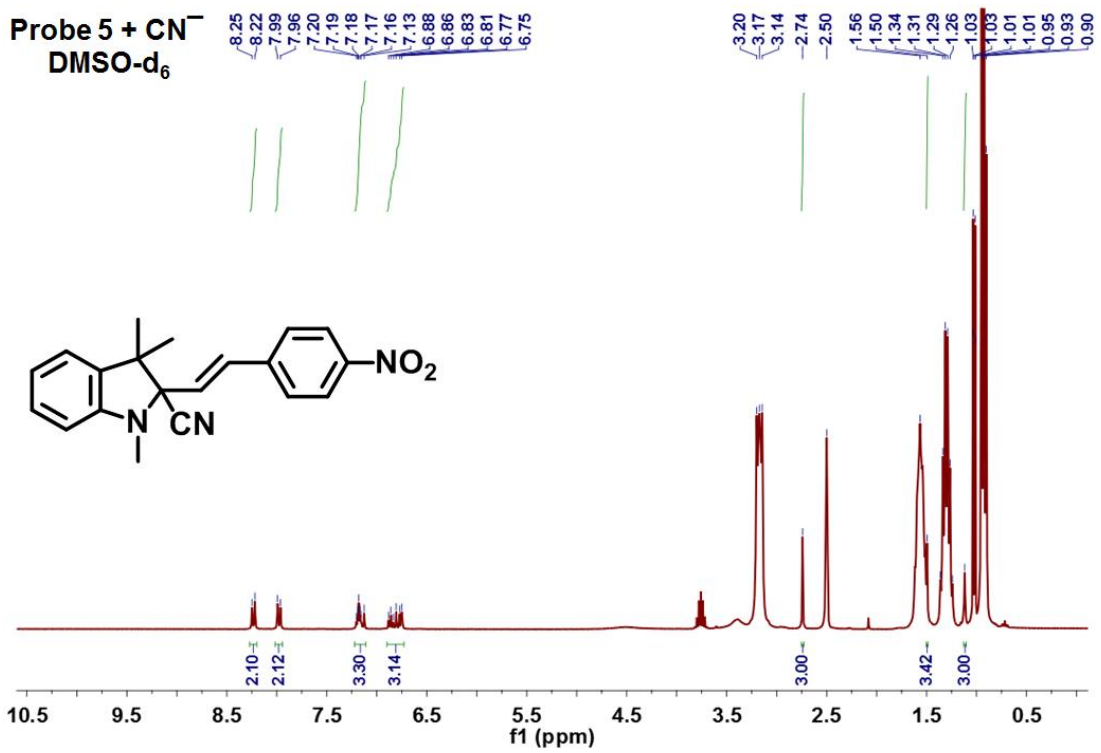

Figure 24. ^{1}H NMR spectra of Probe 5 + CN^{-} in DMSO-d_6.

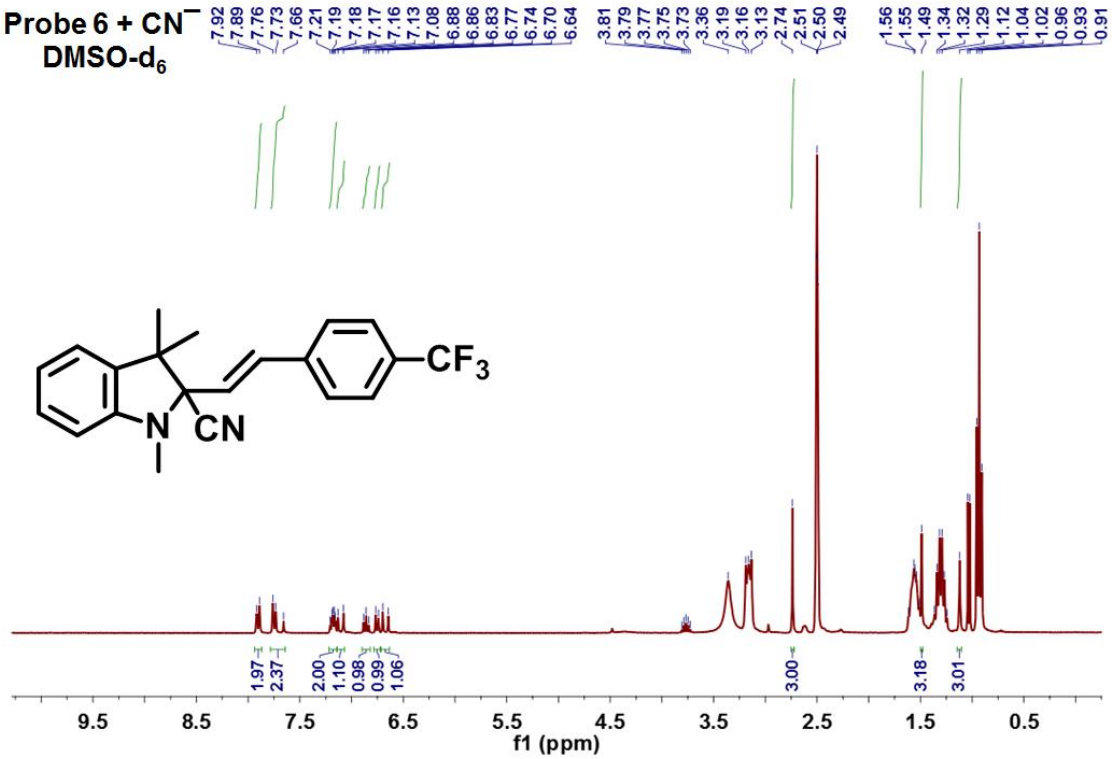

Figure 25. ^{1}H NMR spectra of Probe 6 + CN^{-} in DMSO-d_6.

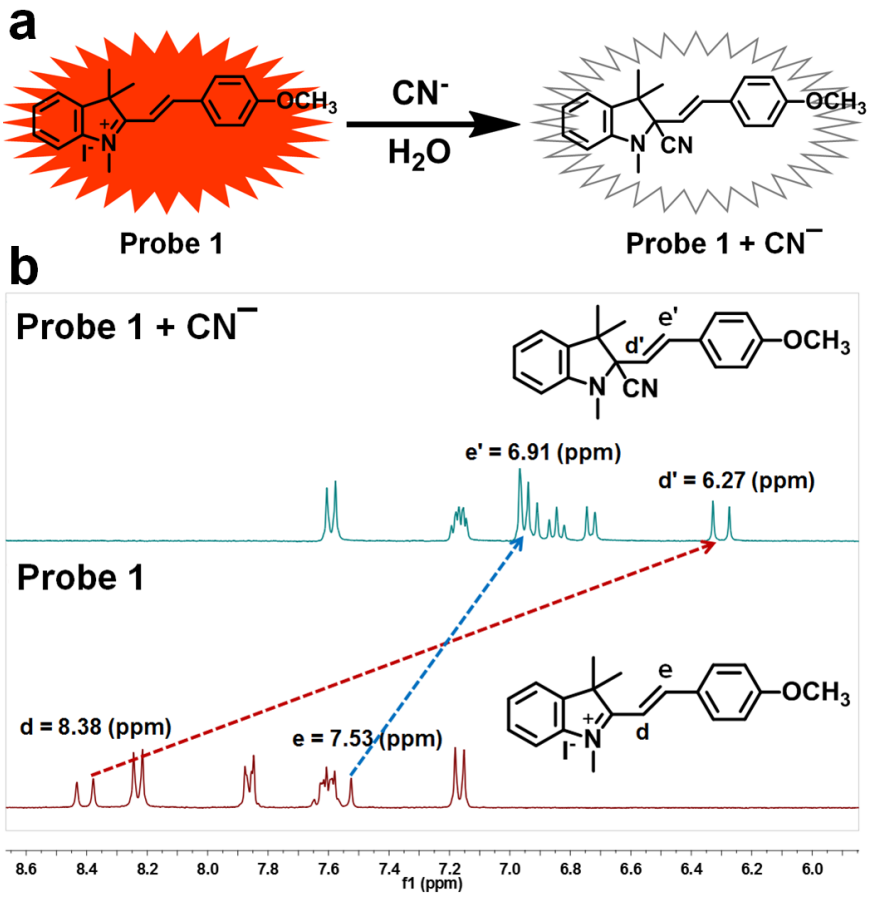

Figure 26. (a) Proposed scheme for conversion of Probe 1 to Probe 1 + CN^- ion; (b) ^1H NMR spectra of Probe 1 and Probe 1 + CN^- in DMSO-d_6. The arrows indicate the chemical shifts of $H_{d/d'}$ (from 8.32 ppm to 6.27 ppm) and $H_{e/e'}$ (from 7.53 ppm to 6.91 ppm).

The polarized C=N bond of the indolium group in cyanine chromophores provides an excellent electron deficient reaction site for CN^- nucleophilic attack.[47-49] As mentioned above, the conjugation between donor and acceptor in probes 1-6 might modulate the intramolecular charge transfer (ICT) state giving rise to large absorbance band changes in the presence of CN^- ion. To further confirm the detection mechanism, NMR titration experiments was performed through the addition of 5 equiv. of tetrabutyl ammonium cyanide (TBACN) to solutions of probes 1-6 in DMSO-d_6 (Figs. 20-25). As shown in Fig. 26, upon addition of CN^- to the solution of probe 1, all of the lower field aromatic peaks shifted upfield; in addition, the initial peaks of ethylene protons H_d (δ = 8.32 ppm) and H_e (δ = 7.53 ppm) disappeared and were replaced by new peaks of $H_{d'}$ (δ = 6.27 ppm) and $H_{e'}$ (δ = 6.91 ppm). Moreover, the original nitrogen methyl proton signal at 4.39 ppm shifted upfield to 2.71 ppm, and the other two methyl proton signals at 1.82 shifted upfield and were split into two peaks (δ = 1.46 ppm and 1.11 ppm) due to the weakened electron-withdrawing character of the indolium group (Fig. 26). Similar phenomena were observed when adding excess TBACN to solutions of probes 1-6 (Figs. 20-25).

Conclusions

In summary, six derivatives of new hemicyanine chromophores based on methylindocyanine were designed and synthesized as novel colorimetric sensors for cyanide ion detection in aqueous medium. Upon treatment with cyanide ions in 100% water, these hybrid hemicyanine probes displayed a notable UV-visible response. The detection of cyanide was realized via the nucleophilic addition of cyanide anion to the indolium group of the hemicyanine chromophores, which resulted in blockage of the intramolecular charge transfer (ICT) process in the sensor and induction of notable transmission changes and a simultaneously observable color change. Furthermore, competitive anions of F^-, Cl^-, Br^-, I^-, AcO^-, HSO_4^-, SCN^-, NO_3^-, and ClO_4^- did not show any significant interference with hemicyanine chromophores in either color or UV-visible intensity, indicating high selectivity for CN^- sensing. Moreover, the CN^- ion limit of detection calculated for probe 1 based on 3σ/slope was 0.36 μM, a considerably lower concentration compared to those of probes 5-6. Furthermore, the sensitivity for the detection of CN^- ions can be controlled by substituents, where electron-donating substituents induced faster reactions compared to electron-withdrawing groups.

References

1. V. Kumar, E.V. Anslyn, J Am Chem Soc, 135(2013) 6338-44.
2. X. Zheng, W. Zhu, D. Liu, H. Ai, Y. Huang, Z. Lu, ACS Appl Mater Interfaces, 6(2014) 7996-8000.
3. D.W. Boening, C.M. Chew, Water, Air, Soil Pollut, 109(1999) 67-79.
4. T.Z. Sadyrbaeva, Sep Purif Technol, 86(2012) 262-5.
5. K. Grossmann, Pest Manag Sci, 66(2010) 113-20.
6. R. Koenig, Science, 287(2000) 1737-8.
7. Y.-R. Chen, L.J. Deterding, K.B. Tomer, R.P. Mason, Biochemistry, 39(2000) 4415-22.
8. T. Tylleskär, W. Howlett, H. Rwiza, S. Aquilonius, E. Stålberg, B. Linden, et al., J Neurol Neurosurg Psychiatry, 56(1993) 638-43.
9. Z. Yan, M. Cai, P.K. Shen, J Mater Chem, 22(2012) 2133-9.
10. J. Jiang, X. Wang, W. Zhou, H. Gao, J. Wu, Phys Chem Chem Phys, 4(2002) 4489-94.
11. C. Giuriati, S. Cavalli, A. Gorni, D. Badocco, P. Pastore, J Chromatogr A, 1023(2004) 105-12.
12. P.R. Fielden, S.J. Smith, J.F. Alder, Analyst, 111(1986) 695-700.
13. R. Rubio, J. Sanz, G. Rauret, Analyst, 112(1987) 1705-8.
14. A. Safavi, N. Maleki, H.R. Shahbaazi, Anal Chim Acta, 503(2004) 213-21.
15. R. Badugu, J.R. Lakowicz, C.D. Geddes, J Am Chem Soc, 127(2005) 3635-41.
16. Z. Xu, X. Chen, H.N. Kim, J. Yoon, Chem Soc Rev, 39(2010) 127-37.
17. C.Y. Kim, S. Park, H.-J. Kim, Dyes Pigm, 130(2016) 251-5.
18. B. Shi, P. Zhang, T. Wei, H. Yao, Q. Lin, Y. Zhang, Chem Commun, 49(2013) 7812-4.
19. S. Goswami, S. Paul, A. Manna, Dalton Trans, 42(2013) 10682-6.
20. W.C. Lin, S.K. Fang, J.W. Hu, H.Y. Tsai, K.Y. Chen, Anal Chem, 86(2014) 4648-52.
21. L. Yang, X. Li, J. Yang, Y. Qu, J. Hua, ACS Appl Mater Interfaces, 5(2013) 1317-26.
22. X. Cheng, R. Tang, H. Jia, J. Feng, J. Qin, Z. Li, ACS Appl Mater Interfaces, 4(2012) 4387-92.
23. M.-J. Peng, Y. Guo, X.-F. Yang, L.-Y. Wang, J. An, Dyes Pigm, 98(2013) 327-32.
24. Y. Wang, S.-H. Kim, Dyes Pigm, 102(2014) 228-33.
25. P. Zhang, B.-B. Shi, T.-B. Wei, Y.-M. Zhang, Q. Lin, H. Yao, et al., Dyes Pigm, 99(2013) 857-62.
26. J.L. Fillaut, H. Akdas-Kilig, E. Dean, C. Latouche, A. Boucekkine, Inorg Chem,

52(2013) 4890-7.

27. F. Huo, J. Kang, C. Yin, J. Chao, Y. Zhang, Sens Actuator B-Chem, 215(2015) 93-8.

28. J. Li, X. Qi, W. Wei, Y. Liu, X. Xu, Q. Lin, et al., Sens Actuator B-Chem, 220(2015) 986-91.

29. J.J. Li, W. Wei, X.L. Qi, X. Xu, Y.C. Liu, Q.H. Lin, et al., Spectrochim Acta Mol Biomol Spectrosc, 152(2016) 288-93.

30. S.-Y. Na, H.-J. Kim, Tetrahedron Lett, 56(2015) 493-5.

31. S. Goswami, A. Manna, S. Paul, A.K. Das, K. Aich, P.K. Nandi, Chem Commun, 49(2013) 2912-4.

32. J. Liu, Q. Lin, H. Yao, M. Wang, Y.-M. Zhang, T.-B. Wei, Chin Chem Lett, 25(2014) 35-8.

33. W.-T. Gong, Q.-L. Zhang, L. Shang, B. Gao, G.-L. Ning, Sens Actuator B-Chem, 177(2013) 322-6.

34. M. Yoo, S. Park, H.-J. Kim, Sens Actuator B-Chem, 220(2015) 788-93.

35. G.R. You, G.J. Park, S.A. Lee, Y.W. Choi, Y.S. Kim, J.J. Lee, et al., Sens Actuator B-Chem, 202(2014) 645-55.

36. X. Lou, L. Qiang, J. Qin, Z. Li, ACS Appl Mater Interfaces, 1(2009) 2529-35.

37. M.R. Ajayakumar, K. Mandal, K. Rawat, D. Asthana, R. Pandey, A. Sharma, et al., ACS Appl Mater Interfaces, 15(2013) 6996-7000.

38. B. Garg, Y.C. Ling, 51(2015) 8809-12.

39. X.-x. Ou, Y.-l. Jin, X.-q. Chen, C.-b. Gong, X.-b. Ma, Y.-s. Wang, et al., Anal Methods, 7(2015) 5239-44.

40. J. Yin, Y. Kwon, D. Kim, D. Lee, G. Kim, Y. Hu, et al., J Am Chem Soc, 136(2014) 5351-8.

41. F. Wang, L. Wang, X. Chen, J. Yoon, Chem Soc Rev, 43(2014) 4312-24.

42. W. Sun, S. Guo, C. Hu, J. Fan, X. Peng, Chem Rev, 116(2016) 7768-817.

43. F.-T. Kong, S.-Y. Dai, K.-J. Wang, Adv Optoelectron, 2007(2007) 1-13.

44. Y.-S. Chen, C. Li, Z.-H. Zeng, W.-B. Wang, X.-S. Wang, B.-W. Zhang, J Mater Chem, 15(2005) 1654-61.

45. J. Yin, Y. Hu, J. Yoon, Chem Soc Rev, 44(2015) 4619-44.

46. W. Sun, J. Fan, C. Hu, J. Cao, H. Zhang, X. Xiong, et al., Chem Commun, 49(2013) 3890-2.

47. L. Yang, X. Li, Y. Qu, W. Qu, X. Zhang, Y. Hang, et al., Sens Actuator B-Chem, 203(2014) 833-47.

48. Y. Sun, Y. Li, X. Ma, L. Duan, Sens Actuator B-Chem, 224(2016) 648-53.

49. T. Liu, F. Huo, J. Li, F. Cheng, C. Yin, Sens Actuator B-Chem, 239(2017) 526-35.

국문 요약

물속에 있는 유해성 음이온을 검출 하는 일은 매우 중요한 일입니다. 많은 유해성 음이온 중 사이아나이드 음이온은 인간과 동물의 심혈관, 호흡기 그리고 중추 신경계에 많은 영향을 주어 심할 경우 죽음에 이르게 하는 위험한 물질입니다. 그렇기 때문에 편리하고 감응성 및 선택성이 좋으며 값싼 사이아나이드 검출 방법의 개발이 요구되어집니다. 그 요구를 충족하기 위해 유기물 분자 기반 화학 센서들이 개발되었습니다. 하지만 물에 잘 녹지 않는 유기물 특성상 많은 분자 기반 화학 센서들을 물에서 이용하는 것은 어렵습니다. 하지만 이번에 합성한 총 6개의 다른 기능성 그룹(-OCH3, -H, 3-vinyl, -CH3, -NO2, 그리고 -CF3)을 가진 헤미사이아닌 기반 화학 센서들은 물에서도 검출이 가능합니다. 합성한 화학 센서들은 수용액 상태에서 사이아나이드 음이온을 선택적 그리고 높은 민감도로 검출하였습니다. 이 화학 센서는 사이아나이드 음이온을 검출 전엔 색깔을 띄다가 검출 후엔 무색으로 바뀌거나 불투명해지는 것을 통하여 비색법을 통하여 검출 여부를 알 수가 있습니다. 그리고 다른 다양한 음이온(F^-, Cl^-, Br^-, I^-, AcO^-, $HSO4^-$, SCN^-, $NO3^-$, and $ClO4^-$)을 넣고 확인한 결과 색깔변화는 나타나지 않았으며, 이를 통해 합성된 케모센서가 선택성이 있다는 걸 확인하였습니다. 추가적으로 6가지의 다른 기능성 그룹들을 이용하여 검출 능력을 확인한 결과 기능성 그룹이 electron-withdrawing group 또는 electron-donating group인지에 따라서 ICT에 변화가 생겨 화학센서의 sensitivity를 조절 가능하다는 것을 확인하였습니다.